

This is the postprint version of the following article: Scarabelli L, Sánchez-Iglesias A, Pérez-Juste J, Liz-Marzán LM. A “Tips and Tricks” Practical Guide to the Synthesis of Gold Nanorods. *The Journal of Physical Chemistry Letters* **2015**;6(21):4270-4279, which has been published in final form at [10.1021/acs.jpcl.5b02123](https://doi.org/10.1021/acs.jpcl.5b02123). This article may be used for non-commercial purposes in accordance with ACS Terms and Conditions for Self-Archiving.

# A “tips ’n tricks” Practical Guide to the Synthesis of Gold Nanorods

Leonardo Scarabelli,<sup>a,\*</sup> Ana Sánchez-Iglesias,<sup>a</sup> Jorge Pérez-Juste,<sup>b</sup> Luis M. Liz-Marzán<sup>a,c,\*</sup>

<sup>a</sup> Bionanoplasmonics Laboratory, CIC biomaGUNE, Paseo de Miramon 182, 20009 Donostia-San Sebastian, Spain

<sup>b</sup> Departamento de Química Física, Universidade de Vigo, 36310 Vigo, Spain

<sup>c</sup> Ikerbasque, Basque Foundation for Science, 48013 Bilbao, Spain

\* **Corresponding authors’ email:** lscarabelli@cicbiomagune.es; llizmarzan@cicbiomagune.es

Gold nanorods have been the first successful example of anisotropic plasmonic nanostructure synthesized by wet-chemistry.<sup>1</sup> Since the early 2000’s, they have received increasing attention because of their tunable optical (plasmonic) properties, which render them ideal candidates for a wide range of applications, such as solar harvesting,<sup>2</sup> photovoltaics,<sup>3</sup> surface enhanced spectroscopies,<sup>4,5</sup> sensing<sup>4,6,7</sup> and therapy,<sup>2,8</sup> to name a few. A direct consequence is that a broad variety of researchers with a wide range of backgrounds are currently interested in exploiting their optical properties. Therefore, fast, easy, scalable and reliable methods for the synthesis of gold nanorods are necessary for their actual implementation in new technologies, which could have a direct impact on our future every-day life. During the past two decades, a huge effort has been made to decrease the size dispersity of colloidal gold nanorods; unfortunately we have not achieved sufficient reproducibility of the synthetic protocols, understood as the possibility of reproducing them in a different working-environment. The reason is that small details and “tricks” are generally left out in the experimental section of dedicated publications.

In this viewpoint article we highlight all the synthetic aspects that generally remain in the shadows, in order to provide the scientific community with a user friendly guide for the production of gold nanorods. We present in **Scheme 1** an informal representation of the optimization of synthesis methods to achieve the required quality.



**Scheme 1.** Optimization of synthesis methods can be achieved through careful tuning of various parameters such as reactants concentrations, which influence thermodynamic and kinetic aspects of seeded growth.

## GENERAL COMMENTS

First of all, we point out some general aspects that must be considered in a wet nanochemistry lab prior to facing the improvement in performance and reproducibility of synthetic procedures.

*-Know your water.* The quality of the water supply used for the synthesis is one of the main sources of irreproducibility. Milli-Q water is deionized and filtered but *not* distilled. As a consequence, the presence of contaminant traces cannot be excluded. Mass spectrometry is an appropriate tool to check water quality, but HPLC grade water can be purchased as a quality standard. Another important water-related parameter is pH, which can dramatically influence the aspect ratio of your nanorods (see below). It should be noted that pH may be different even after Milli-Q purification, meaning that re-optimization may be required, typically through systematic tuning of  $\text{AgNO}_3$  concentration (in our laboratories water pH ranges between 5 and 5.5).

*-Chemical Supplier.* Many of the chemicals used in nanosynthesis may include different possible contaminant traces, depending upon brand and batch. Every synthesis paper should thus report the supplier name as well as the purity of each chemical, and attention should be paid to this

information when trying to reproduce a published protocol. In the specific case of Au nanorod synthesis, CTAB purity is the main issue: back in 2008, Smith and Korgel demonstrated that the same synthesis in the same laboratory can result in a completely different product by simply changing the CTAB supplier.<sup>9,10</sup>

*-Glassware cleaning.* Although this may seem obvious, it is important that the entire lab environment be kept clean, but particular care should be taken when cleaning the glassware. Each piece must be washed first with soap and water, then soaked in *aqua regia* (*ca.* 10 min), rinsed thoroughly with water, washed with Milli-Q water and dried. Vials using caps with internal metallic surface should be avoided, as this is a potential source of contamination.

*-Store the stock solutions.* A common practical way to organize and speed-up your work is the preparation of stock solutions for each reagent. Therefore, it is essential to keep record of the preparation date of every stock solution, as well as proper storage conditions. If aimed for Au nanorod synthesis, CTAB can be stored for long periods of time, simply avoiding high temperatures, but for AgNO<sub>3</sub> and ascorbic acid we recommend the preparation of fresh stock solutions after a maximum of 7 days, storage in the fridge (4 °C) and in a darkened beaker for protection against light. Additionally, when handling a silver salt, contact with any metallic instrument should be avoided (use a plastic spatula, or the wide side of a Pasteur pipette to weigh it). Tetrachloroauric acid (HAuCl<sub>4</sub>) is a hygroscopic salt: a convenient way to prepare a stock solution is to use the entire content of the sealed bottle, weighing the full and empty container to calculate the exact mass. The stock can then be split in glass vials (*ca.* 10 mL) and stored in the fridge, protected from sunlight, for a long period of time (>12 months). However, stock solutions should be discarded if visible changes are observed (dark lid for AgNO<sub>3</sub>, yellowish color for ascorbic acid, insoluble material for HAuCl<sub>4</sub>).

## **GOLD NANOROD SYNTHESIS STEP BY STEP**

The mechanism behind the formation of Au nanorods is still a matter of much interest, since a general mechanistic model would allow us to identify specific guidelines for the design of a synthetic pathway for each nanostructure.<sup>11-14</sup> Xia's group recently published a highly informative perspective article dealing with the distinction between thermodynamic and kinetic control during crystal growth.<sup>15</sup> An entire section of this paper is dedicated to the symmetry breaking event, a necessary step in the development of anisotropic structures, such as nanorods. The main message is that stabilization of crystallographic facets and anisotropic growth are different issues, the former being under thermodynamic control and the latter under kinetic control. Keeping this consideration

in mind, it is not surprising that Au nanorod synthesis requires both thermodynamic and kinetic control, which significantly increases the number of parameters that should be taken into account. This can be easily seen by simply considering that a gold nanoparticle colloid can be described by the average diameter alone, while description of Au nanorods should include length, thickness, aspect ratio, reduction-yield (how much precursor gets reduced) and shape-yield (the proportion of formed particles that are nanorods). This consideration is translated in practice into the need for a higher degree of control throughout the growth process, which is of particular relevance when the goal is not simply the production of high-quality nanorods, but also a tight control on the actual aspect ratio to be produced.

The historical turning point in the development of efficient nanorod wet synthesis methods was the introduction of the so called seeded-growth protocol, where nucleation is performed separately to prepare the seeds, which are subsequently added to the growth solution for nanorod production.<sup>16</sup> In fact, the conditions required for controlled growth are opposite to those needed for homogenous nucleation, thereby allowing us to avoid the formation of new nuclei during the growth step. It is worth mentioning here that even though so-called ‘seedless’ methods have been reported, they are generally characterized by a lower product-quality and reproducibility. Furthermore, these methods require the addition of small amounts of a strong reducing agent, typically sodium borohydride, which leads to the *in situ* formation of seeds through partial reduction of the gold salt precursor into Au(0). It is also important to decide whether you wish to prepare single crystalline or pentatwinned Au nanorods. Although both are rod-like nanoparticles, they have different dimensions, surface facets, twin defects, geometry, crystallographic habit and even composition. Pentatwinned nanorods display a pentagonal cross-section, with [100] lateral facets, and [111] facets closing the crystal at the tips, they typically have larger dimensions and higher aspect ratios, with longitudinal bands in the NIR range, and are synthesized by growth on citrate capped twinned seeds under “silver-free” conditions.<sup>17</sup> On the other hand, single crystal nanorods display smaller dimensions and aspect ratios, the longitudinal plasmon band can be finely tuned from the visible into the NIR, and are grown using CTAB capped single crystal seeds, in the presence of silver nitrate.<sup>18</sup> There has been some controversy regarding their crystallographic habit, but it seems to be accepted by now that they show octagonal cross-section and high-index [520] lateral facets.<sup>19</sup> All together, these considerations impose significant differences in the respective synthetic protocols, each with different critical issues, which we analyze point by point in the discussion below. We analyze separately the various components of a typical gold nanorod synthesis. All the discussions in this viewpoint paper are summarized in the Experimental section (Supporting Information), where we

provide four detailed protocols for the synthesis of single crystalline and pentatwinned nanorods that are used in our lab on a daily basis.

**The Seeds.** In the context of this work, seeds are small nuclei (typically below 5 nm) made of gold, which serve as the starting point for the development of a more complex (anisotropic) structure.<sup>14,20</sup> It is thus obvious that a high quality seed solution is necessary to obtain high quality nanorods. Ideally, the seeds should be monodisperse and display the same crystallographic habit, which in practice is achieved by adding a strong reducing agent in excess (typically sodium borohydride, NaBH<sub>4</sub>, 6-60 equivalent),<sup>21</sup> as fast as possible and under vigorous stirring. As a tip, when preparing a seed solution you should picture in your mind an *instantaneous* addition of the reductant to achieve the *simultaneous* production of all nuclei, homogeneously distributed in the *entire solution volume*. Moreover, it is important to remember that NaBH<sub>4</sub> is hygroscopic, and can react with the water contained in the air; therefore, it is important to weigh it as fast as possible and to prepare it fresh every time. Two types of seeds can be used depending on the type of nanorods to be prepared: CTAB capped seeds are used for single crystal nanorods and citrate capped seeds for pentatwinned nanorods. The former are single crystalline (**Figure 1B**), with an average diameter below 2 nm, and their solutions appear light brown, *i.e.* they do not show any localized surface plasmon resonance (LSPR) band (**Figure 1A**); a red-pink shade would indicate the formation of bigger particles, which are likely to compromise the quality of the final product. Even though seeds are highly reactive, they can be stored between 27 and 29 °C for a couple of hours, which may also help to complete decomposition of the remaining borohydride ions. Citrate capped seeds are slightly bigger (*ca.* 3.5 nm on average) and therefore present the typical red color of Au colloids, with an LSPR band centered around 507 nm (**Figure 1A**). Their larger dimensions also enhance their stability up to few days if stored in the fridge. It is important to point out that a mixture of crystallographic habits are usually obtained, comprising single crystalline, monotwinned and pentatwinned populations (**Figure 1C**), which has a major impact on the usual low shape-yield in the synthesis of pentatwinned Au nanorods, typically around 30 %.

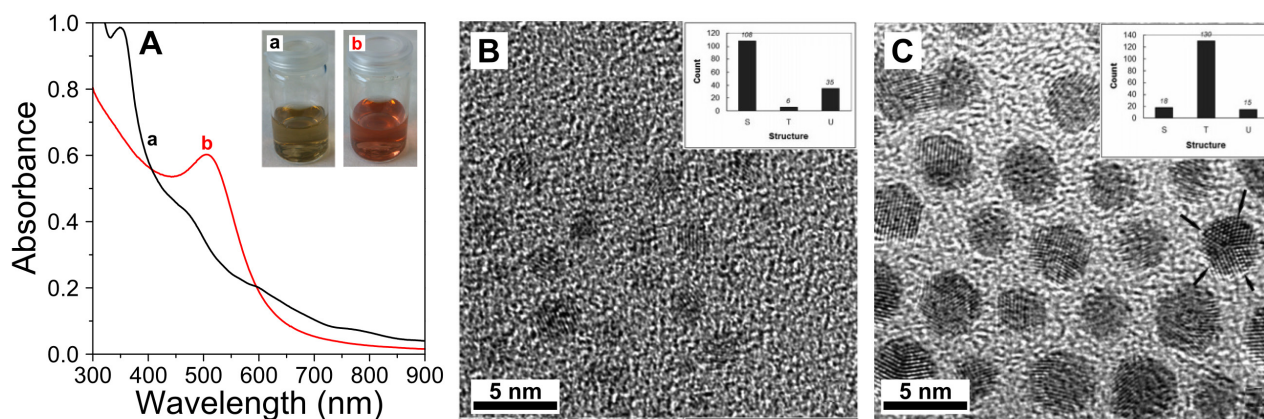


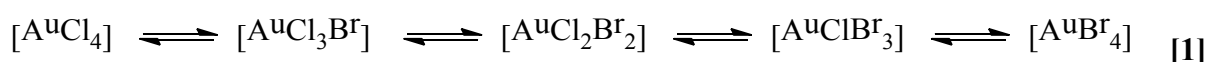
**Figure 1. Au seeds for the synthesis of single crystal and pentatwinned Au nanorods. A:** UV-vis spectra of CTAB coated (a, black line) and citrate coated (b, red line) seeds. **Inset:** picture of a typical seed solution: CTAB coated (a, left) and citrate coated (b, right). **B-C:** High resolution transmission electron micrograph of single crystalline seed@CTAB and pentatwinned seed@citrate, respectively; the histograms show the counting for single crystal (S), twinned (T) and undefined (U) seeds. Adapted from Ref. [22].

**The surfactant.** The choice of CTAB as a suitable surfactant for the synthesis of Au nanorods stems from the wealth of existing literature dealing with the rheology and phase behavior of CTAB solutions, since at suitable concentrations CTAB was known to form rod-shaped micelles, which were expected to induce anisotropic growth on spherical seeds.<sup>23–27</sup> This view slowly evolved into the hypothesis that CTAB acted as a face-specific capping agent: in the subsequent two decades numerous studies have been conducted with the aim of understanding the role of the surfactant on anisotropic growth, changing tail length<sup>28</sup> and head group<sup>16</sup> or using gemini surfactants,<sup>29,30</sup> among other variations; interestingly, several research groups came to the conclusion that the bromide counterion has a more important role in the anisotropic growth than the surfactant itself. Even though CTAB remains the most employed surfactant, we can identify three basic requirements to achieve rod-like shape:

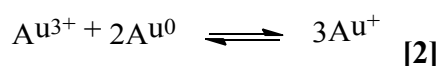
- A quaternary ammonium surfactant head group that forms a complex with the gold salt precursor and modifies its redox potential.
- The presence of bromide as counter-ion, since any attempt to synthesize single crystalline nanorods in either CTAC or BDAC alone failed unless minute amounts of bromide ions (*ca.* 1 mM) are added to the reaction mixture, suggesting a key role of bromide ions in the symmetry breaking process.<sup>31</sup>

- A carbon tail that is long enough to stabilize the nanorods, but short enough to achieve solubility close to room temperature.<sup>32</sup>

**The gold precursor.** Tetrachloroauric acid,  $\text{HAuCl}_4$ , is widely used in gold nanoparticle synthesis. Therefore, three different oxidation states are involved: Au(III) in the precursor, Au(I) as intermediate, and Au(0) comprising the nanoparticles.<sup>33</sup> Au(III) is a d8 soft metal center, forming square planar complexes. According to Ligand Field Theory, the complexation strength of Au(III) with halide ions follows the series:  $\text{I}^- > \text{Br}^- > \text{Cl}^-$ . Therefore, in the presence of CTAB the four chloride ligands in  $\text{AuCl}_4^-$  will be eventually replaced by bromide ions from the surfactant:



which is reflected in a color change from pale yellow to dark-orange yellow, with a final absorption maximum at 396 nm.<sup>34</sup> Additionally, the  $\text{AuBr}_4^-$  ions will form an ion-pair with the quaternary ammonium surfactant monomers which are neutral and therefore insoluble in water, requiring a surfactant concentration with a 60:1 ratio to ensure dissolution.<sup>18</sup> Both the  $\text{AuCl}_4^-$  to  $\text{AuBr}_4^-$  ligand exchange and the  $\text{AuBr}_4^-$ -CTA complex formation will influence their redox potentials, which are cathodically shifted.<sup>35</sup> Such a variation in the redox potentials will influence the growth kinetics. Taking all this into account, it is important to ensure not only that the gold salt has been completely dissolved, but also that ligand exchange has been completed. Moreover, an additional equilibrium needs to be considered between all three Au oxidation states, which can be pushed towards comproportionation or disproportionation reactions, depending on the relative stability of each species in the mixture:



In the growth solution, the most stable species is Au(I), meaning that the equilibrium is displaced towards the comproportionation between Au(III) and Au(0), *i.e.* Au nanorods (or other Au nanoparticles) will be oxidized in the presence of Au(III).<sup>34-37</sup> In this scenario, a central role is played by the reducing agent, as discussed below.

**The reductant.** One of the key points in the seeded growth method is the use of a weak reducing agent, so that gold reduction takes place only on existing nuclei in solution, which also act as catalysts. Even though other reducing agents have been proposed,<sup>38,39</sup> the most popular choice is still ascorbic acid.<sup>40,41</sup> Upon addition of ascorbic acid to a growth solution containing a mixture of  $\text{HAuCl}_4$  and CTAB, the reduction of Au(III) to Au(I) takes place, indicated by the solution turning

colorless (the ligand-to-metal charge transfer band disappears for a  $d^{10}$  metal center as Au(I)). This is in fact an important step as it guarantees that when the seeds are injected into this growth solution their oxidation by the favorable comproportion reaction (see above) is avoided. It is also crucial that the reducing agent *cannot* complete the reduction of Au(I) into Au(0), *i.e.* secondary nucleation during the growth step is prevented. In fact, the seeds act as catalysts for the final reduction step, thereby inducing reduction of the Au(I) precursor on their surface only. Two possible mechanisms have been proposed: **(1)** a disproportionation reaction catalyzed by the seeds produces Au(0) and Au(III) (eq. [2] from left to right), the latter immediately being reduced again into Au(I) by remaining reductant,<sup>42-44</sup> and **(2)** the Au(0) surface drains electrons from the reductant and catalyzes the *in situ* reduction of Au(I).<sup>18,45</sup> It should be noted that ascorbic acid features a pH-dependent reduction potential, being lower under acidic conditions and higher at more basic pH values,<sup>46</sup> which has been applied to modulate Au nanorod growth. In fact, if the pH is above 9 ascorbic acid will be able to reduce Au(I) into Au(0), even in the absence of seeds, thus compromising the seeded-growth mechanism.

Finally, another important issue involving the reductant is the reduction-yield. In fact, it is still unclear if the gold precursor is entirely reduced on the surface of the growing rods, and otherwise why this is the case.<sup>47,48</sup> In order to measure the reduction-yield in a more convenient way, it is useful to employ a simple spectroscopic analytical method based on the absorbance of light with a wavelength of 400 nm, which can be measured with a simple UV-vis spectrometer.<sup>35,49</sup> The idea is to select a wavelength where the main contribution to absorbance comes from absorption related to interband transitions in metallic gold,<sup>50,51</sup> which would thus be used to determine the amount of gold precursor that has been reduced, regardless of particle size and shape (note that large particles will display strong scattering so the accuracy of this method would be compromised in this case). We recently reported an experimental validation of this method for citrate-capped seeds,<sup>34</sup> but the validity of this relationship for Au nanorods can also be demonstrated by numerical calculations (based on the boundary element method, BEM<sup>52</sup>) of the extinction spectra of nanorods with different aspect ratios and dimensions (**Figure 2**). When the simulated spectra were normalized by particle volume (**Figure 2A**), the extinction cross section (equivalent in practice to absorbance) at 400 nm was found to be identical for all geometries. We thus plotted (**Figure 2B**) the absorbance at 400 nm as a function of nanorod volume, obtaining a perfectly linear relationship. This clearly demonstrates that all Au nanoparticles with the same volume will equally contribute to the measured absorbance at 400 nm. It is worth mention here that deviation from this relationship can be observed for large particles, since then the scattering contribution to the extinction cross-section becomes significant. To further confirm the experimental evidences we characterized several gold

nanorod samples with different volumes and aspect ratios by UV-vis spectroscopy and ICP-MS elemental analysis. As can be seen in **Figure 2C**, the variation of absorbance at 400 nm for the different samples with the corresponding Au concentration determined by ICP-MS follows a linear trend with a slope of 2.4. Therefore, a value of 1.2 for the absorbance at 400 nm corresponds to an  $\text{Au}^0$  concentration of 0.5 mM. Noteworthy, an absorbance at 400 nm below the expected value would indicate that part of the Au precursor remained in solution as Au(I), which in turn results in slow reshaping and spectral blue shift, as has been reported by many groups, when nanorods are aged for long periods of time. A simple centrifugation step can be used to remove the excess of reagents and enhance the long term stability of Au nanorods (even for years). We estimate the theoretical expected absorbance of a 0.5 mM solution of “nanometric” Au(0) starting from the value of extinction cross-section (for volume unity) that we obtained from the calculations:

$$A = -\text{Log}_{10} e^{-L\sigma\tau} \quad [3]$$

where L is the optical path length (nm),  $\sigma$  is the scattering cross-section of a gold volumetric unity ( $\text{nm}^2$ ), and  $\tau$  is the volume fraction of gold ( $\text{nm}^{-3}$ ). Using equation [3] we obtained a predicted absorbance of 1.1, in good agreement with the experimental value of 1.2. Overall, calculation and ICP-MS data confirm that:

- The reduction yield can be precisely estimated from the absorbance at 400 nm, regardless of the shape and size of the nanoparticles.
- An absorbance of 1.2 corresponds to  $[\text{Au}^0] = 0.5 \text{ mM}$  (not accurate for larger particles, see above).
- During a standard Au nanorod preparation there is *quantitative reduction* of the Au precursor.

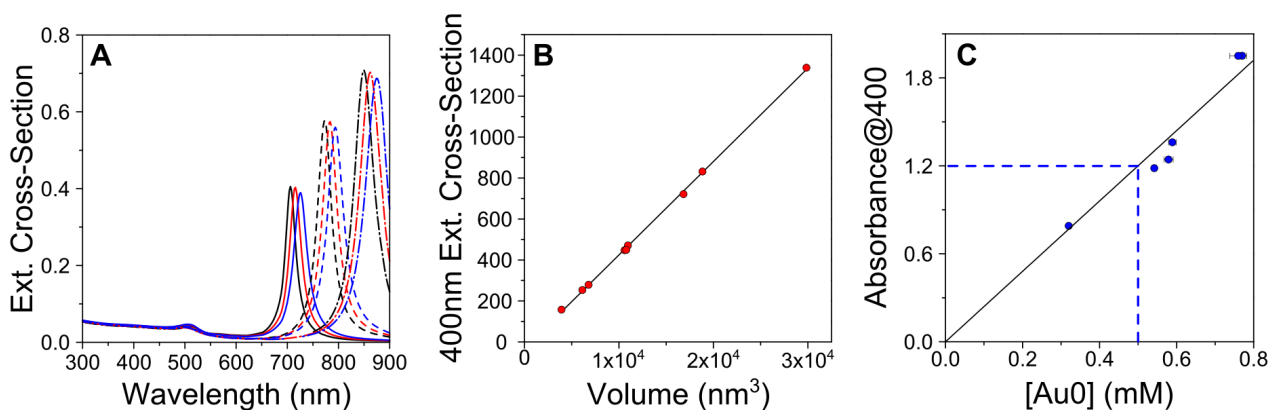


**Figure 2. Reduction-yield in Au nanorod synthesis. A:** Calculated extinction spectra for Au

nanorods of different aspect ratios and dimensions, normalized to the particle volume: AR = 3 (solid lines): 50x16.7 nm (black), 60x20 nm (red), 70x23.3 nm (blue); AR = 4 (dotted lines): 50x12.5 nm (black), 60x15 nm (red), 70x17.5 nm (blue); AR = 5 (dash-dotted lines): 50x10 nm (black), 60x12 nm (red), 70x14 nm (blue). Note that the absorbance at 400 nm is constant for all spectra. **B**: value of the extinction cross-section at 400 nm plotted against particle volume; the solid line is a linear interpolation to the data, with a Pearson's coefficient  $R^2 > 0.999$ . **C**: value of the absorbance at 400 nm of different Au nanorod colloids plotted against  $[Au^0]$  obtained from ICP-MS analysis. The solid black line is a linear fit to the data, obtained by imposing a null y-intercept, with a Pearson's coefficient  $R^2 > 0.994$ . The blue lines confirm the relationship:  $A_{400nm} = 1.2 \Leftrightarrow [Au^0] = 0.5 \text{ mM}$ .

**Growth kinetics.** The growth of Au nanorods is characterized in general by a slow kinetics, meaning that several hours are needed to complete particle growth. Interestingly, significant differences can be found between pentatwinned and single crystal nanorods, thus involving different growth mechanisms. In the case of pentatwinned Au nanorods a constant red shift of the longitudinal plasmon band is observed during growth, suggesting a gradual increase in aspect ratio throughout the entire growth process (**Figure 3A,B**).<sup>18</sup> Single crystal nanorods on the other hand display a more complicated behavior in which we can distinguish three different stages (**Figure 3C,D**): initially the plasmon band redshifts quickly as the gold salt gets reduced (**1**), but then blueshifts (**2**), and the blueshift continues even after reduction is completed (**3**).<sup>34,53</sup> TEM analysis at the different stages (**Figure 3e-g**) revealed that the growing particles initially display a dumbbell-like morphology but then reshape into "perfect" rods at the later growth stage; calculations demonstrate that such a reshaping can explain the blueshift of the longitudinal plasmon band.<sup>53,54</sup> Assuming that reduction takes place predominantly on the region of highest surface energy, *i.e.* at the tips of the growing rods, the freshly reduced Au atoms should migrate along the surface to form the most thermodynamically stable crystallographic habit. At a reaction temperature of 30 °C this process can take several hours to be completed.<sup>15</sup>

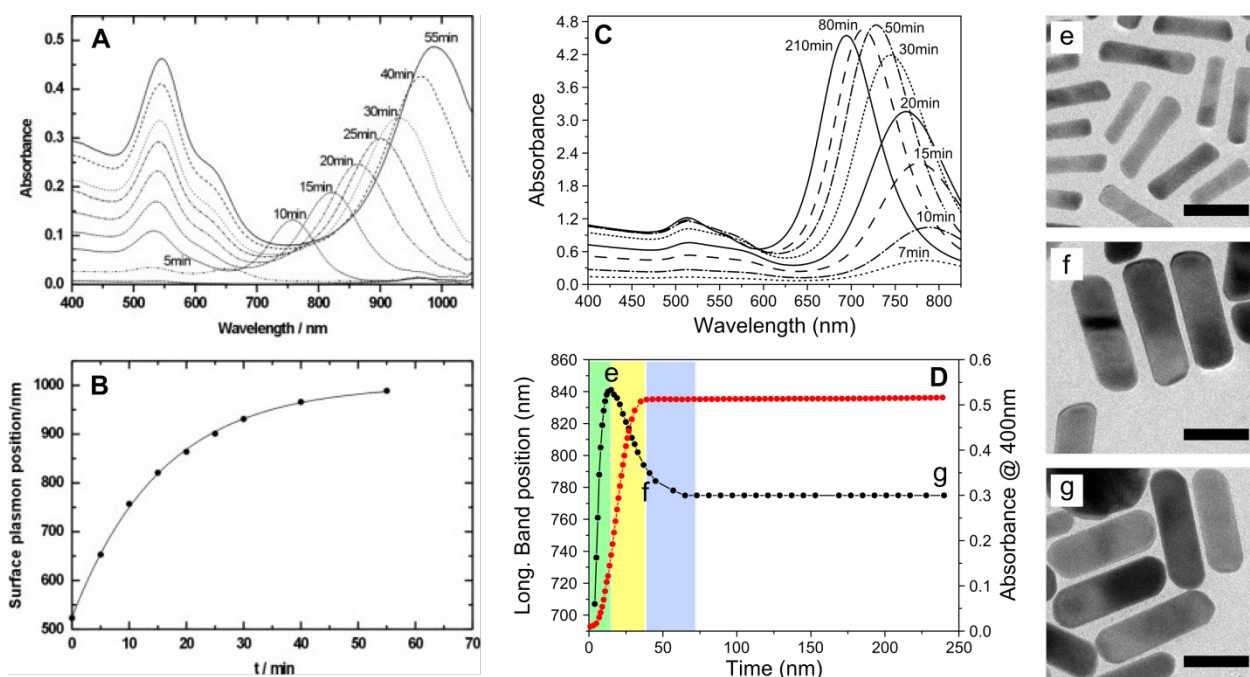


**Figure 3. Kinetic optical study of Au nanorod synthesis.** **A:** UV-vis-NIR spectra of growing pentatwinned Au nanorods in solution. **B:** position of the longitudinal LSPR band as a function of time (adapted from Ref. [18]). **C:** UV-vis-NIR spectra of growing single crystal Au nanorods in solution. **D:** position of the longitudinal LSPR band (black) and value of the absorbance at 400 nm (red), as a function of time; three different stages are distinguished: redshift and reduction (green), blueshift and reduction (yellow) and blueshift no reduction (blue). **e-g:** TEM images of growing nanorods at different growth stages, as indicated in **D**: at the maximum redshift of the longitudinal LSPR band (**e**), at the end of reduction (**f**), at the end of growth (**g**) (adapted from Ref. [34]).

**Silver ions.** The specific role of silver ions in the synthesis of single crystal Au nanorods remains unclear. Three main mechanisms have been proposed: (1) under potential deposition, (2) formation of a  $\text{Ag}[\text{BrCTA}]_2$  complex that acts as a face-specific capping agent on the lateral facets of the growing seeds and (3) modification of CTAB micelle formation through silver-bromide interactions.<sup>22,24,31,55,56</sup> We deliberately leave out of this paper a detailed mechanistic study of the role of the silver, but rather concentrate our attention toward its practical consequences on synthetic protocols. The presence of  $\text{Ag}^+$  ions is essential for the synthesis of single crystal Au nanorods, while it hinders the anisotropic growth of pentatwinned nanorods. In the latter case, the absence of silver as a surface active agent renders metal reduction “less” selective for nanorod tips. A lower temperature is thus required to slow down the reduction and diffusion of reduced atoms on the surface of the growing particles: typically, pentatwinned Au nanorods are synthesized at 20 °C,

which in turn imposes a limitation on the maximum CTAB concentration that can be used (8 mM vs. 100 mM for single crystal Au nanorods). On the contrary, for single crystal Au nanorods, the presence of silver simultaneously leads to higher selectivity for reduction on the tips (kinetically influencing the symmetry breaking) and stabilization of lateral facets (thermodynamically stabilizing the final product). In fact, Au nanorods can be synthesized at a much higher temperature, but moderate reaction temperatures are usually selected, again to slow down the reduction and achieve a narrower size distribution.

**Additives.** A recent trend in the Au nanorods community is the use of additional chemicals to improve the quality of the material and the tunability of the synthetic protocol. The nature of these additives (also known as co-factors) ranges from inorganic anions or cations to both aromatic and aliphatic molecules. In this context, Murray and co-workers proposed the use of both salicylic and oleic acid, which allowed them to reach a wider range of aspect ratios and dimensions while maintaining a narrow size dispersion.<sup>57-59</sup> In both cases the authors proposed a mechanism related to the intercalation of the additive within the CTAB bilayer surrounding the growing particles, which would increase its stiffness and therefore improve control over the symmetry breaking event. It is however important to realize that these additives can also interact in various other ways with the chemicals present in the growth medium. In a related study, we demonstrated that salicylic acid can reduce Au(III) into Au(I), and this can be used as a pre-reduction step to tune the final aspect ratio of the nanorods (see Experimental Section).<sup>34</sup> It should also be noted that, the carboxylic group can alter the solution pH and form complexes with the gold precursor, thereby influencing its reduction potential.<sup>41,46</sup>

**Purification.** The shape-yield obtained after seeded growth is not always sufficient for the targeted applications, in particular when high quality optical properties are important. This is particularly bad for pentatwinned nanorods, which are typically obtained with a shape-yield below 30%. Several purification methods have been proposed,<sup>60</sup> including centrifugation,<sup>61</sup> electrophoresis,<sup>62</sup> selective oxidation<sup>63</sup> and depletion interaction forces.<sup>64-66</sup> Among these, the latter presents numerous advantages, as it can be readily scaled up, it is both shape and size selective, relatively fast and highly efficient. Depletion forces are attractive in nature but their origin is not particularly intuitive. They arise when colloidal particles are suspended at low concentration, in the presence of a more abundant population of smaller solutes (termed “depletant”), which are excluded from the space in between the larger particles, thereby reducing configurational entropy. In a nanoparticle colloidal suspension, surfactant micelles can be used as the depletant, creating an attractive force defined as:

$$|U| = \frac{2 \cdot r_m \cdot A \cdot N_{AV} \cdot (C - C_{cmc})}{AN} k_B T \quad [4]$$

where  $r_m$ ,  $C_{cmc}$ ,  $C$  and  $AN$  are the radius, the critical micelle concentration, the analytical concentration and the aggregation number of the surfactant,  $N_{AV}$  is Avogadro's number, and  $A$  is the area of interaction between two adjacent particles. In this way, nanoparticles with different size and shape can be selectively precipitated by changing the concentration of the surfactant.<sup>67</sup> **Figure 4** exemplifies the purification of both pentatwinned and single crystal Au nanorods, showing that the less anisotropic by-product (spheres and decahedra for pentatwinned rods and spheres or cubes for single crystal ones) can be separated overnight in a single purification step.

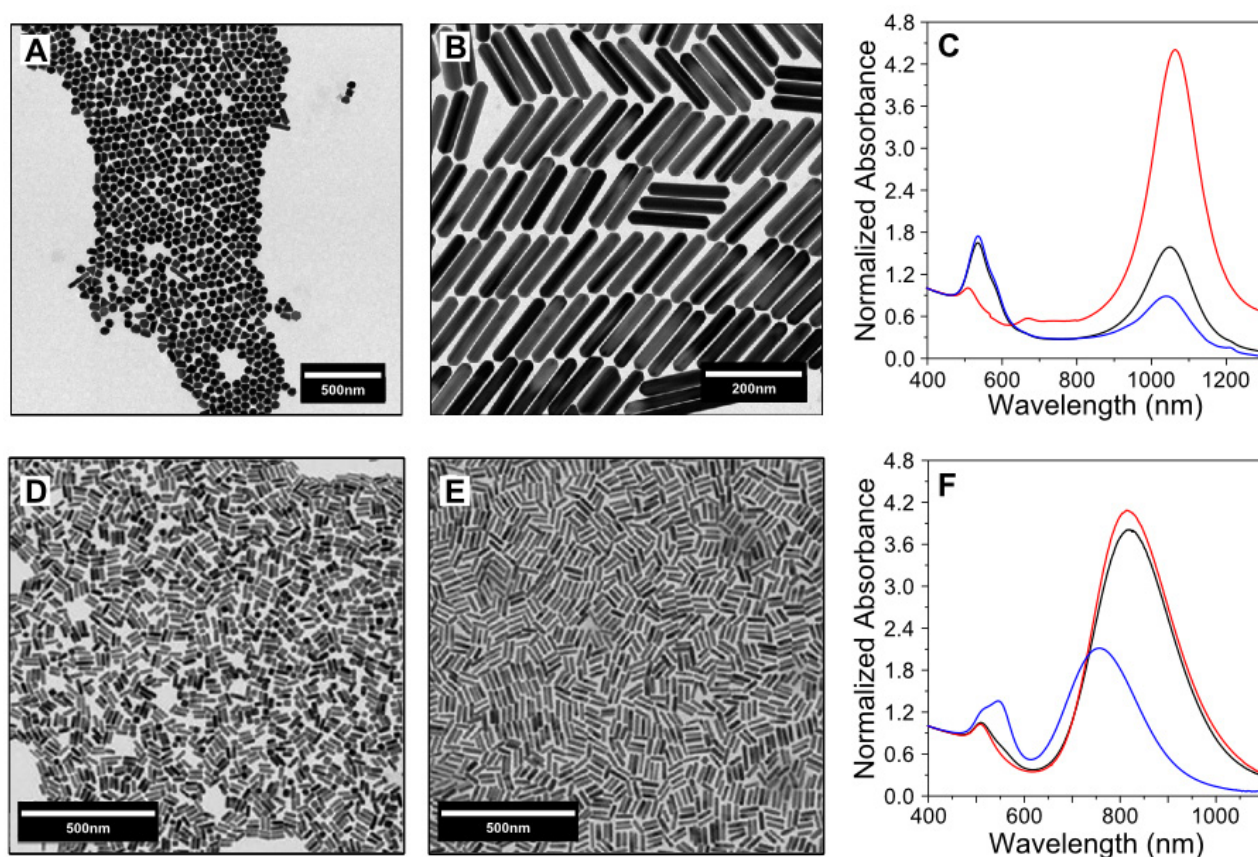


**Figure 4. Purification of Au nanorod colloids via depletion forces.** **A:** TEM image from the supernatant containing the synthesis by-product for pentatwinned rods. **B:** TEM image of purified pentatwinned Au nanorods; adapted from Ref. [68]. **C:** UV-vis-NIR analysis of the purification of pentatwinned Au nanorods, 16 hours after addition of CTAC solution: original product (black curve), supernatant (blue curve) and purified nanorods (red curve). **D:** TEM image from the supernatant containing the synthesis by-product for single crystal Au nanorods. **E:** TEM image of purified single crystal rods. **F:** UV-vis-NIR analysis of the purification of single crystal nanorods, 2 hours after redispersion in CTAB solution. The color code is the same as that in C.

**Characterization.** The main techniques required for Au nanorod characterization are UV-vis-NIR spectroscopy and TEM. It is important to realize that they are complementary to each other and both of them should be used in all cases. In our opinion, there is a general tendency to overestimate the amount of information that can be derived from TEM analysis, and often optical data are neglected or even completely omitted. In practice, an optical spectrum can tell to an expert eye much more than a TEM image (**Figure 5**): the full width at half maximum (FWHM) and the shape of the longitudinal LSPR band are excellent measures of size dispersion, while the plasmon band position gives us a quick estimate of the average aspect ratio, the nanoparticles concentration can be derived from the absorbance at 400 nm and the ratio between the maximum absorbance of the longitudinal and transverse LSPR bands, as well as the presence of a shoulder on the transverse band, are indications of the presence of by-products (**Figure 5A**). On the other hand, a TEM image can provide the particle dimensions with high accuracy, but if a fair reproduction of the three-dimensional morphology is required electron tomography should be employed.<sup>69</sup> It is also important to realize that a single TEM image is not the best way to demonstrate the absence of by-products, since shape segregation has been reported to occur during drying, meaning that the by-product will largely concentrate on a particular area of the grid (**Figure 5B-C**).<sup>70,71</sup> It should be taken into account that, in order to obtain sufficient TEM statistics for the length, thickness and aspect ratio of nanorods, several images must be analyzed, ideally at different magnifications.<sup>72</sup> It is important to mention in this respect that small angle X-ray scattering (SAXS) allows us to estimate the dimension of nanorods directly from the solution, analyzing billions of particles, and if complemented with small angle neutron scattering (SANS) it is also possible to investigate the ligand layer surrounding the particles.<sup>73,74</sup> Finally, the preparation method of TEM specimens also deserves attention. The first important issue is the concentration of the surfactant, which should be kept just below the cmc: hand shaking of the solution usually leads to bubble formation, but they should quickly disappear. Secondly, the concentration of nanorods must be optimized: generally, the sample should be concentrated to achieve an absorbance at 400 nm around 2.4. Finally, longer drying times often result in a better organization of the nanorods on the grid.<sup>75,76</sup> A tip: place the TEM grid on parafilm<sup>®</sup> and deposit 5-10  $\mu\text{L}$  of the nanorod colloid: the hydrophobicity of the surface will prevent the drop from splashing, it will dry slowly on the grid within a couple of hours, ensuring a uniform distribution of nanorods (**Figure 5B**).

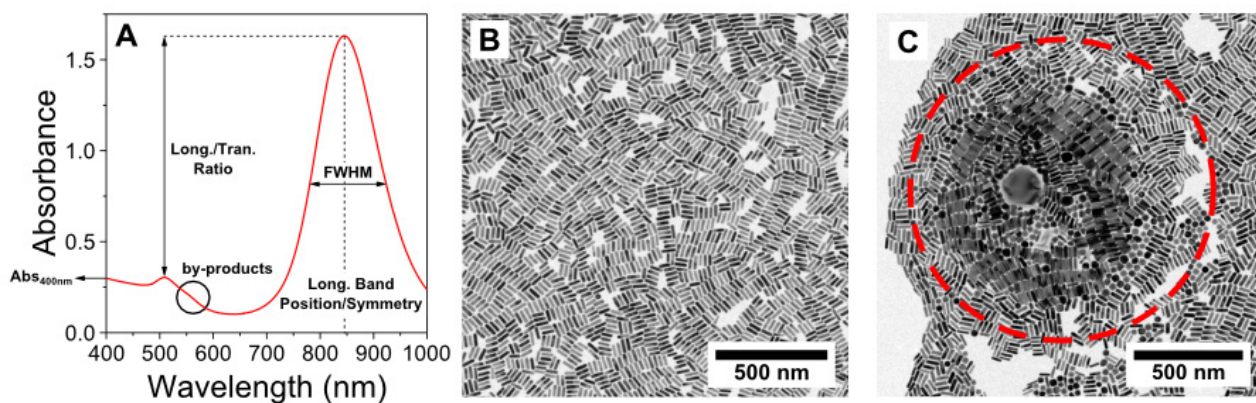


**Figure 5. UV-vis-NIR vs. TEM characterization.** **A:** Typical UV-vis-NIR spectrum of a single crystal Au nanorod colloid. In the image we indicate the parameters that are indicative of product quality. **B-C:** TEM images from the same TEM grid, showing the accumulation of isotropic material at a certain spot (red dotted circle). It is important to notice that the shape-yield that can be estimated from **B** and **C** is significantly different, *both being biased*.

## IMPORTANT CONSIDERATIONS

We highlight in this section selected take-home messages that we consider important when dealing with the synthesis of Au nanorods.

- *Importance of showing raw UV-vis-NIR data.* UV-vis-NIR spectra provide a lot of information: not only they reflect the quality of the material, but can also help others to reproduce the synthesis. It is crucial in this respect to indicate whether the spectra have been normalized and if so which was the normalization criterion, but keeping in mind that the original raw spectrum can provide a reasonable estimate of Au nanorod concentration through the absorbance at 400 nm.
- *A nice TEM image does not necessarily indicate high shape-yield.* A TEM image alone is not a sufficient indication of sample size dispersion and purity! It is necessary to acquire several images at different magnifications, as well as registering the corresponding UV-vis-NIR spectrum, which can also be used to assess the presence or absence of by-products.
- *Do you really need the perfect rods?* Significant amounts of time and effort can be saved in the preparation of the “perfect Au nanorod colloid” if we know what we really need for our project. Just to give an example: if the nanorods will be drop-casted on a substrate, plasmon coupling is expected, so it probably makes little sense to search for very low FWHM in the

colloid. The same principle applies before deciding if a purification step is needed: no matter which synthetic protocol you follow and how precisely you reproduce it, a certain amount of by-products with different shapes will invariably be present along with your nanorods. It is thus important to be sure if a 100% pure Au nanorod colloid is really needed. Even if for a pentatwinned Au nanorod synthesis a shape-yield of 30% almost invariably requires purification, for single crystal nanorods 90% purity can be readily achieved.

- *Optimizing a protocol in your lab.* In case you need to optimize a published protocol to your needs, here are some general rules to keep in mind.
  - [Ag<sup>+</sup>]: a higher concentration will increase the aspect ratio (for single crystal rods only).<sup>77</sup>
  - [ascorbic acid]: a higher concentration will decrease the aspect ratio.<sup>77</sup>
  - [seed]: a lower amount of seed will result in the production of larger nanorods, in general with a smaller aspect ratio.<sup>78</sup>
  - [pH]: lower pH values will slow down the growth kinetics, leading to higher aspect ratios.<sup>79</sup>

The synthesis of Au nanorods relies on the ratios between all reagents involved. For this reason the allowed range for each component is quite narrow, so we recommend to modify multiple parameters rather than a single one.<sup>78</sup>

- *Larger volumes? ...not so easy.* Scaling-up a synthesis method is not a trivial task! We are faced with two major problems: diffusion and temperature. The first one is related with the mixing rate of reagents: upon seed addition the growing particles should be uniformly distributed in the solution; this is a very different job when dealing with 10 mL or with 2 L of solution, and can significantly affect the quality of the product. Second, temperature is extremely important in Au nanorod synthesis. When preparing the initial CTAB solution one is usually tempted to warm it up so as to speed-up its dissolution, but cooling down a large volume of water takes time; be sure that the entire solution reaches the desired temperature before starting the growth. We suggest to start synthesizing small volumes of solution (around 10 mL) to verify the quality of water and the stock solutions, and then face scaled-up synthesis.

## OUTLOOK

- Although Au nanorods display many advantages as compared to other nanostructures, an important drawback is the difficulty in removing the protective CTAB bilayer.<sup>80</sup> Even though many procedures for successful surfactant removal can be found in the literature, an obvious alternative would be a CTA<sup>+</sup>-free synthesis of Au nanorods.

- Pentatwinned Au nanorods may be advantageous for some applications, as they display higher aspect ratios and better defined crystallographic habit, do not contain silver, etc. There is however a strong limitation in the shape-yield, meaning that the development of a better seeded-growth protocol is still necessary, which may be related to a better control of seed production.
- The development of flow reactors for reproducible nanorod synthesis would have a large impact on the industrial production and implementation of nanoparticles.<sup>15</sup> These systems can greatly enhance control over reaction kinetics, thereby increasing the tunability of the existing protocols, and expanding our possibilities in the design of new nanostructures.<sup>81</sup> Even though millifluidic systems have been proposed for Au nanorod synthesis, there is still room to achieve acceptable levels of morphological and optical tunability.<sup>82</sup>

## Quotes

“Know your water. The quality of the water supply used for the synthesis is one of the main sources of irreproducibility.”

“Au nanorod synthesis requires both thermodynamic and kinetic control, which significantly increases the number of parameters that should be taken into account.”

“When preparing a seed solution you should picture in your mind an *instantaneous* addition of the reductant to achieve the *simultaneous* production of all nuclei, homogeneously distributed in the *entire solution volume*.”

“It is crucial that the reducing agent *cannot* complete the reduction of Au(I) into Au(0), *i.e.* secondary nucleation during the growth step is prevented.”

“Au nanoparticles with the same volume will equally contribute to the measured absorbance at 400 nm.”

“UV-vis-NIR spectroscopy and TEM are complementary to each other and both of them should be used for Au nanorod characterization in all cases.”

## Acknowledgements

This work was supported by the European Research Council (PLASMAQUO, 267867) and by the Spanish MINECO (MAT2013-45168-R and MAT2013-46101-R).

**Supporting Information Available:** Detailed description of the experimental details for the synthesis of several types of Au nanorods.

## REFERENCES:

- (1) Huang, X.; Neretina, S.; El-Sayed, M. A. Gold Nanorods: From Synthesis and Properties to Biological and Biomedical Applications. *Adv. Mater.* **2009**, *21*, 4880–4910.
- (2) de Aberasturi, D. J.; Serrano-Montes, A. B.; Liz-Marzán, L. M. Modern Applications of Plasmonic Nanoparticles: From Energy to Health. *Adv. Opt. Mater.* **2015**, *3*, 602–617.
- (3) Atwater, H. A.; Polman, A. Plasmonics for Improved Photovoltaic Devices. *Nat. Mater.* **2010**, *9*, 205–213.
- (4) Langer, J.; Novikov, S. M.; Liz-Marzán, L. M. Sensing Using Plasmonic Nanostructures and Nanoparticles. *Nanotechnology* **2015**, *26*, 322001.
- (5) Lal, S.; Grady, N. K.; Kundu, J.; Levin, C. S.; Lassiter, J. B.; Halas, N. J. Tailoring Plasmonic Substrates for Surface Enhanced Spectroscopies. *Chem. Soc. Rev.* **2008**, *37*, 898–911.
- (6) Vigderman, L.; Khanal, B. P.; Zubarev, E. R. Functional Gold Nanorods: Synthesis, Self-Assembly, and Sensing Applications. *Adv. Mater.* **2012**, *24*, 4811–4841.
- (7) Hamon, C.; Liz-Marzán, L. M. Hierarchical Assembly of Plasmonic Nanoparticles. *Chem. - Eur. J.* **2015**, *21*, 9956–9963.
- (8) Webb, J. A.; Bardhan, R. Emerging Advances in Nanomedicine with Engineered Gold Nanostructures. *Nanoscale* **2014**, *6*, 2502–2530.
- (9) Smith, D. K.; Korgel, B. A. The Importance of the CTAB Surfactant on the Colloidal Seed-Mediated Synthesis of Gold Nanorods. *Langmuir* **2008**, *24*, 644–649.
- (10) Rayavarapu, R. G.; Ungureanu, C.; Krystek, P.; van Leeuwen, T. G.; Manohar, S. Iodide Impurities in Hexadecyltrimethylammonium Bromide (CTAB) Products: Lot–Lot Variations and Influence on Gold Nanorod Synthesis. *Langmuir* **2010**, *26*, 5050–5055.
- (11) Lohse, S. E.; Burrows, N. D.; Scarabelli, L.; Liz-Marzán, L. M.; Murphy, C. J. Anisotropic Noble Metal Nanocrystal Growth: The Role of Halides. *Chem. Mater.* **2013**, 34–43.
- (12) Langille, M. R.; Personick, M. L.; Zhang, J.; Mirkin, C. A. Defining Rules for the Shape Evolution of Gold Nanoparticles. *J. Am. Chem. Soc.* **2012**, *134*, 14542–14554.
- (13) Niu, W.; Zhang, L.; Xu, G. Seed-Mediated Growth of Noble Metal Nanocrystals: Crystal Growth and Shape Control. *Nanoscale* **2013**, *5*, 3172–3181.
- (14) Grzelczak, M.; Pérez-Juste, J.; Mulvaney, P.; Liz-Marzán, L. M. Shape Control in Gold Nanoparticle Synthesis. *Chem. Soc. Rev.* **2008**, *37*, 1783–1791.
- (15) Xia, Y.; Xia, X.; Peng, H.-C. Shape-Controlled Synthesis of Colloidal Metal Nanocrystals: Thermodynamic versus Kinetic Products. *J. Am. Chem. Soc.* **2015**, 7947–7966.
- (16) Nikoobakht, B.; El-Sayed, M. A. Preparation and Growth Mechanism of Gold Nanorods (NRs) Using Seed-Mediated Growth Method. *Chem. Mater.* **2003**, *15*, 1957–1962.
- (17) Johnson, C. J.; Dujardin, E.; Davis, S. A.; Murphy, C. J.; Mann, S. Growth and Form of Gold Nanorods Prepared by Seed-Mediated, Surfactant-Directed Synthesis. *J. Mater. Chem.* **2002**, *12*, 1765–1770.
- (18) Pérez-Juste, J.; Liz-Marzán, L. M.; Carnie, S.; Chan, D. Y. C.; Mulvaney, P. Electric-Field-Directed Growth of Gold Nanorods in Aqueous Surfactant Solutions. *Adv. Funct. Mater.* **2004**, *14*, 571–579.
- (19) Carbó-Argibay, E.; Rodríguez-González, B.; Gómez-Graña, S.; Guerrero-Martínez, A.; Pastoriza-Santos, I.; Pérez-Juste, J.; Liz-Marzán, L. M. The Crystalline Structure of Gold Nanorods Revisited: Evidence for Higher-Index Lateral Facets. *Angew. Chem. Int. Ed.* **2010**, *49*, 9397–9400.
- (20) Gole, A.; Murphy, C. J. Seed-Mediated Synthesis of Gold Nanorods: Role of the Size and Nature of the Seed. *Chem. Mater.* **2004**, *16*, 3633–3640.

- (21) Carregal-Romero, S.; Pérez-Juste, J.; Hervés, P.; Liz-Marzán, L. M.; Mulvaney, P. Colloidal Gold-Catalyzed Reduction of Ferrocyanate (III) by Borohydride Ions: A Model System for Redox Catalysis. *Langmuir* **2010**, *26*, 1271–1277.
- (22) Liu, M.; Guyot-Sionnest, P. Mechanism of Silver(I)-Assisted Growth of Gold Nanorods and Bipyramids. *J. Phys. Chem. B* **2005**, *109*, 22192–22200.
- (23) Lin, Z.; Cai, J. J.; Scriven, L. E.; Davis, H. T. Spherical-to-Wormlike Micelle Transition in CTAB Solutions. *J. Phys. Chem.* **1994**, *98*, 5984–5993.
- (24) Murphy, C. J.; Thompson, L. B.; Chernak, D. J.; Yang, J. A.; Sivapalan, S. T.; Boulos, S. P.; Huang, J.; Alkilany, A. M.; Sisco, P. N. Gold Nanorod Crystal Growth: From Seed-Mediated Synthesis to Nanoscale Sculpting. *Curr. Opin. Colloid Interface Sci.* **2011**, *16*, 128–134.
- (25) Esumi, K.; Matsuhisa, K.; Torigoe, K. Preparation of Rodlike Gold Particles by UV Irradiation Using Cationic Micelles as a Template. *Langmuir* **1995**, *11*, 3285–3287.
- (26) Jana, N. R. Gram-Scale Synthesis of Soluble, Near-Monodisperse Gold Nanorods and Other Anisotropic Nanoparticles. *Small* **2005**, *1*, 875–882.
- (27) Jana, N. R.; Gearheart, L.; Murphy, C. J. Seed-Mediated Growth Approach for Shape-Controlled Synthesis of Spheroidal and Rod-like Gold Nanoparticles Using a Surfactant Template. *Adv. Mater.* **2001**, *13*, 1389–1393.
- (28) Gao, J.; Bender, C. M.; Murphy, C. J. Dependence of the Gold Nanorod Aspect Ratio on the Nature of the Directing Surfactant in Aqueous Solution. *Langmuir* **2003**, *19*, 9065–9070.
- (29) Guerrero-Martínez, A.; Pérez-Juste, J.; Carbó-Argibay, E.; Tardajos, G.; Liz-Marzán, L. M. Gemini-Surfactant-Directed Self-Assembly of Monodisperse Gold Nanorods into Standing Superlattices. *Angew. Chem. Int. Ed.* **2009**, *48*, 9484–9488.
- (30) Esumi, K.; Hara, J.; Aihara, N.; Usui, K.; Torigoe, K. Preparation of Anisotropic Gold Particles Using a Gemini Surfactant Template. *J. Colloid Interface Sci.* **1998**, *208*, 578–581.
- (31) Almora-Barrios, N.; Novell-Leruth, G.; Whiting, P.; Liz-Marzán, L. M.; López, N. Theoretical Description of the Role of Halides, Silver, and Surfactants on the Structure of Gold Nanorods. *Nano Lett.* **2014**, *14*, 871–875.
- (32) Si, S.; Leduc, C.; Delville, M.-H.; Lounis, B. Short Gold Nanorod Growth Revisited: The Critical Role of the Bromide Counterion. *ChemPhysChem* **2012**, *13*, 193–202.
- (33) Edgar, J. A.; McDonagh, A. M.; Cortie, M. B. Formation of Gold Nanorods by a Stochastic “Popcorn” Mechanism. *ACS Nano* **2012**, *6*, 1116–1125.
- (34) Scarabelli, L.; Grzelczak, M.; Liz-Marzán, L. M. Tuning Gold Nanorod Synthesis through Prereduction with Salicylic Acid. *Chem. Mater.* **2013**, *25*, 4232–4238.
- (35) Rodríguez-Fernández, J.; Pérez-Juste, J.; Mulvaney, P.; Liz-Marzán, L. M. Spatially-Directed Oxidation of Gold Nanoparticles by Au(III)–CTAB Complexes. *J. Phys. Chem. B* **2005**, *109*, 14257–14261.
- (36) Carbó-Argibay, E.; Rodríguez-González, B.; Pacifico, J.; Pastoriza-Santos, I.; Pérez-Juste, J.; Liz-Marzán, L. M. Chemical Sharpening of Gold Nanorods: The Rod-to-Octahedron Transition. *Angew. Chem. Int. Ed.* **2007**, *46*, 8983–8987.
- (37) Carbó-Argibay, E.; Rodríguez-González, B.; Pastoriza-Santos, I.; Pérez-Juste, J.; Liz-Marzán, L. M. Growth of Pentatwinned Gold Nanorods into Truncated Decahedra. *Nanoscale* **2010**, *2*, 2377–2383.
- (38) Vigderman, L.; Zubarev, E. R. High-Yield Synthesis of Gold Nanorods with Longitudinal SPR Peak Greater than 1200 Nm Using Hydroquinone as a Reducing Agent. *Chem. Mater.* **2013**, *25*, 1450–1457.
- (39) Newman, J. D. S.; Blanchard, G. J. Formation of Gold Nanoparticles Using Amine Reducing Agents. *Langmuir* **2006**, *22*, 5882–5887.
- (40) Khan, Z.; Singh, T.; Hussain, J. I.; Hashmi, A. A. Au(III)–CTAB Reduction by Ascorbic Acid: Preparation and Characterization of Gold Nanoparticles. *Colloids Surf. B Biointerfaces* **2013**, *104*, 11–17.
- (41) Zümreoglu-Karan, B. A Rationale on the Role of Intermediate Au(III)–vitamin C Complexation in the Production of Gold Nanoparticles. *J. Nanoparticle Res.* **2008**, *11*, 1099–1105.
- (42) Ojea-Jiménez, I.; Romero, F. M.; Bastús, N. G.; Puntès, V. Small Gold Nanoparticles Synthesized with Sodium Citrate and Heavy Water: Insights into the Reaction Mechanism. *J. Phys. Chem. C* **2010**, *114*, 1800–1804.

- (43) Gammons, C. H.; Yu, Y.; Williams-Jones, A. E. The Disproportionation of gold(I) Chloride Complexes at 25 to 200°C. *Geochim. Cosmochim. Acta* **1997**, *61*, 1971–1983.
- (44) Kumar, S.; Gandhi, K. S.; Kumar, R. Modeling of Formation of Gold Nanoparticles by Citrate Method†. *Ind. Eng. Chem. Res.* **2007**, *46*, 3128–3136.
- (45) Rodríguez-Fernández, J.; Pérez-Juste, J.; García de Abajo, F. J.; Liz-Marzán, L. M. Seeded Growth of Submicron Au Colloids with Quadrupole Plasmon Resonance Modes. *Langmuir* **2006**, *22*, 7007–7010.
- (46) Gramlich, G.; Zhang, J.; Nau, W. M. Increased Antioxidant Reactivity of Vitamin C at Low pH in Model Membranes. *J. Am. Chem. Soc.* **2002**, *124*, 11252–11253.
- (47) Orendorff, C. J.; Murphy, C. J. Quantitation of Metal Content in the Silver-Assisted Growth of Gold Nanorods. *J. Phys. Chem. B* **2006**, *110*, 3990–3994.
- (48) Lohse, S. E.; Murphy, C. J. The Quest for Shape Control: A History of Gold Nanorod Synthesis. *Chem. Mater.* **2013**, *25*, 1250–1261.
- (49) Hendel, T.; Wuithschick, M.; Kettemann, F.; Birnbaum, A.; Rademann, K.; Polte, J. In Situ Determination of Colloidal Gold Concentrations with UV–Vis Spectroscopy: Limitations and Perspectives. *Anal. Chem.* **2014**, *86*, 11115–11124.
- (50) Rao, P.; Doremus, R. Kinetics of Growth of Nanosized Gold Clusters in Glass. *J. Non-Cryst. Solids* **1996**, *203*, 202–205.
- (51) Sau, T. K.; Murphy, C. J. Seeded High Yield Synthesis of Short Au Nanorods in Aqueous Solution. *Langmuir* **2004**, *20*, 6414–6420.
- (52) García de Abajo, F. J. Relativistic Electron Energy Loss and Electron-Induced Photon Emission in Inhomogeneous Dielectrics. *Phys. Rev. Lett.* **1998**, *80*, 5180–5183.
- (53) Park, K.; Drummy, L. F.; Wadams, R. C.; Koerner, H.; Nepal, D.; Fabris, L.; Vaia, R. A. Growth Mechanism of Gold Nanorods. *Chem. Mater.* **2013**, *25*, 555–563.
- (54) Grzelczak, M.; Sánchez-Iglesias, A.; Rodríguez-González, B.; Alvarez-Puebla, R.; Pérez-Juste, J.; Liz-Marzán, L. M. Influence of Iodide Ions on the Growth of Gold Nanorods: Tuning Tip Curvature and Surface Plasmon Resonance. *Adv. Funct. Mater.* **2008**, *18*, 3780–3786.
- (55) Jackson, S. R.; McBride, J. R.; Rosenthal, S. J.; Wright, D. W. Where’s the Silver? Imaging Trace Silver Coverage on the Surface of Gold Nanorods. *J. Am. Chem. Soc.* **2014**, *136*, 5261–5263.
- (56) Hubert, F.; Testard, F.; Spalla, O. Cetyltrimethylammonium Bromide Silver Bromide Complex as the Capping Agent of Gold Nanorods. *Langmuir* **2008**, *24*, 9219–9222.
- (57) Dong, A.; Chen, J.; Vora, P. M.; Kikkawa, J. M.; Murray, C. B. Binary Nanocrystal Superlattice Membranes Self-Assembled at the Liquid–air Interface. *Nature* **2010**, *466*, 474–477.
- (58) Ye, X.; Jin, L.; Caglayan, H.; Chen, J.; Xing, G.; Zheng, C.; Doan-Nguyen, V.; Kang, Y.; Engheta, N.; Kagan, C. R.; et al. Improved Size-Tunable Synthesis of Monodisperse Gold Nanorods through the Use of Aromatic Additives. *ACS Nano* **2012**, *6*, 2804–2817.
- (59) Ye, X.; Gao, Y.; Chen, J.; Reifsnnyder, D. C.; Zheng, C.; Murray, C. B. Seeded Growth of Monodisperse Gold Nanorods Using Bromide-Free Surfactant Mixtures. *Nano Lett.* **2013**, 2163–2171.
- (60) Kowalczyk, B.; Lagzi, I.; Grzybowski, B. A. Nanoseparations: Strategies for Size And/or Shape-Selective Purification of Nanoparticles. *Curr. Opin. Colloid Interface Sci.* **2011**, *16*, 135–148.
- (61) Xiong, B.; Cheng, J.; Qiao, Y.; Zhou, R.; He, Y.; Yeung, E. S. Separation of Nanorods by Density Gradient Centrifugation. *J. Chromatogr. A* **2011**, *1218*, 3823–3829.
- (62) Xu, X.; Caswell, K. K.; Tucker, E.; Kabisatpathy, S.; Brodhacker, K. L.; Scrivens, W. A. Size and Shape Separation of Gold Nanoparticles with Preparative Gel Electrophoresis. *J. Chromatogr. A* **2007**, *1167*, 35–41.
- (63) Khanal, B. P.; Zubarev, E. R. Purification of High Aspect Ratio Gold Nanorods: Complete Removal of Platelets. *J. Am. Chem. Soc.* **2008**, *130*, 12634–12635.
- (64) Mao, Y.; Cates, M. E.; Lekkerkerker, H. N. W. Depletion Force in Colloidal Systems. *Phys. Stat. Mech. Its Appl.* **1995**, *222*, 10–24.
- (65) Park, K.; Koerner, H.; Vaia, R. A. Depletion-Induced Shape and Size Selection of Gold Nanoparticles. *Nano Lett.* **2010**, *10*, 1433–1439.
- (66) Jana, N. R. Nanorod Shape Separation Using Surfactant Assisted Self-Assembly. *Chem. Commun.* **2003**, *15*, 1950–1951.

- (67) Scarabelli, L.; Coronado-Puchau, M.; Giner-Casares, J. J.; Langer, J.; Liz-Marzán, L. M. Monodisperse Gold Nanotriangles: Size Control, Large-Scale Self-Assembly, and Performance in Surface-Enhanced Raman Scattering. *ACS Nano* **2014**, *8*, 5833–5842.
- (68) Mayer, M.; Scarabelli, L.; March, K.; Altantzis, T.; Tebbe, M.; Kociak, M.; Bals, S.; García de Abajo, F. J.; Fery, A.; Liz-Marzán, L. M. Controlled Living Nanowire Growth: Precise Control over the Morphology and Optical Properties of AgAuAg Bimetallic Nanowires. *Nano Lett.* **2015**, *15*, 5427–5437.
- (69) Bals, S.; Goris, B.; Liz-Marzán, L. M.; Van Tendeloo, G. Three-Dimensional Characterization of Noble-Metal Nanoparticles and Their Assemblies by Electron Tomography. *Angew. Chem. Int. Ed.* **2014**, *53*, 10600–10610.
- (70) Lekkerkerker, H. N. W.; Tuinier, T. *Colloids and the Depletion Interaction*; Springer, 2011.
- (71) Sánchez-Iglesias, A.; Grzelczak, M.; Pérez-Juste, J.; Liz-Marzán, L. M. Binary Self-Assembly of Gold Nanowires with Nanospheres and Nanorods. *Angew. Chem. Int. Ed.* **2010**, *49*, 9985–9989.
- (72) Murphy, C. J.; Buriak, J. M. Best Practices for the Reporting of Colloidal Inorganic Nanomaterials. *Chem. Mater.* **2015**, *27*, 4911–4913.
- (73) Hubert, F.; Testard, F.; Thill, A.; Kong, Q.; Tache, O.; Spalla, O. Growth and Overgrowth of Concentrated Gold Nanorods: Time Resolved SAXS and XANES. *Cryst. Growth Des.* **2012**, *12*, 1548–1555.
- (74) Gómez-Graña, S.; Hubert, F.; Testard, F.; Guerrero-Martínez, A.; Grillo, I.; Liz-Marzán, L. M.; Spalla, O. Surfactant (Bi)Layers on Gold Nanorods. *Langmuir* **2012**, *28*, 1453–1459.
- (75) Hamon, C.; Postic, M.; Mazari, E.; Bizien, T.; Dupuis, C.; Even-Hernandez, P.; Jimenez, A.; Courbin, L.; Gosse, C.; Artzner, F.; et al. Three-Dimensional Self-Assembling of Gold Nanorods with Controlled Macroscopic Shape and Local Smectic B Order. *ACS Nano* **2012**, *6* (5), 4137–4146.
- (76) Hamon, C.; Novikov, S. M.; Scarabelli, L.; Solís, D. M.; Altantzis, T.; Bals, S.; Taboada, J. M.; Obelleiro, F.; Liz-Marzán, L. M. Collective Plasmonic Properties in Few-Layer Gold Nanorod Supercrystals. *ACS Photonics* **2015**, DOI: 10.1021/acsp Photonics.5b00369.
- (77) Pérez-Juste, J.; Pastoriza-Santos, I.; Liz-Marzán, L. M.; Mulvaney, P. Gold Nanorods: Synthesis, Characterization and Applications. *Coord. Chem. Rev.* **2005**, *249*, 1870–1901.
- (78) Ward, C. J.; Tronndorf, R.; Eustes, A. S.; Auad, M. L.; Davis, E. W. Seed-Mediated Growth of Gold Nanorods: Limits of Length to Diameter Ratio Control. *J. Nanomater.* **2014**, *2014*, 765618–765624.
- (79) Wei, Q.; Ji, J.; Shen, J. pH Controlled Synthesis of High Aspect-Ratio Gold Nanorods. *J. Nanosci. Nanotechnol.* **2008**, *8*, 5708–5714.
- (80) Vigderman, L.; Manna, P.; Zubarev, E. R. Quantitative Replacement of Cetyl Trimethylammonium Bromide by Cationic Thiol Ligands on the Surface of Gold Nanorods and Their Extremely Large Uptake by Cancer Cells. *Angew. Chem. Int. Ed.* **2012**, *51*, 636–641.
- (81) Xia, X.; Xie, S.; Liu, M.; Peng, H.-C.; Lu, N.; Wang, J.; Kim, M. J.; Xia, Y. On the Role of Surface Diffusion in Determining the Shape or Morphology of Noble-Metal Nanocrystals. *Proc. Natl. Acad. Sci.* **2013**, *110*, 6669–6673.
- (82) Lohse, S. E.; Eller, J. R.; Sivapalan, S. T.; Plews, M. R.; Murphy, C. J. A Simple Millifluidic Benchtop Reactor System for the High-Throughput Synthesis and Functionalization of Gold Nanoparticles with Different Sizes and Shapes. *ACS Nano* **2013**, *7*, 4135–4150.